λ_o = vacuum wave length of light
ν_p = frequency observed by particle
ν_i = incident frequency
ν_s = scattered frequency
Ω_R = solid angle at aperture
θ = angle between incident and scattered wave

LITERATURE CITED

1. Yeh, Y., and H. Z. Cummins, *Appl. Phys. Letters*, **4**, 176 (1964).
2. Cummins, H. Z., N. Knable, and Y. Yeh, *Phys. Rev. Letters*, **12**, 150 (1964).
3. Foreman, J. W., Jr., E. W. George, and R. D. Lewis, *Appl. Phys. Letters*, **7**, 77 (1965).
4. ———, E. W. George, J. L. Jetton, R. D. Lewis, J. R. Thornton, and H. J. Watson, Inst. Elec. Electron Eng. J. Quantum Electron, **2**, 260 (1966).
5. Foreman, J. W. Jr., R. D. Lewis, J. R. Thornton, and H. J. Watson, Proc. Inst. Elec. Electron Eng., **54**, 424 (1966).
6. Welch, N. E. and W. J. Tomme, paper presented at Am. Inst. Aeron. Astronaut. meeting (1966).
7. James. R. N., H. S. Siefert, and W. R. Babcock, Am. Inst. Aeron. Astronaut. Paper no. 66-522 presented at Los Angeles (June 26, 1966).
8. Goldstein, R.S., and D. K. Kreid, *paper 67-APM-37 Am. Soc. Mech. Eng., Appl. Mech. Conf.*, Pasadena (June 26, 1967).
9. ———, and W. F. Hagen, *J. Phys. Fluids*, **10**, 1349 (1967).
10. Siegman, A. E., Proc. Inst. Elec. Electron. Eng., **54**, 1350 (1966).
11. Atkinson, B., K. Zdzislaw, and J. M. Smith, *AIChE J.*, **13**, 17 (1967).
12. Christiansen, E. B., and H. E. Lemmon, *ibid.*, **11**, 995 (1965).
13. Sparrow, E. M., S. H. Lin, and T. S. Lundgren, *J. Phys. Fluids*, **7**, 338 (1964).
14. Dealy, J. M., *AIChE J.*, **11**, 745 (1965).
15. Tanner, M. J., and R. I. Manton, *ibid.*, **12**, 816 (1966).
16. Wang, Y. L., and P. A. Longwell, *ibid.*, **10**, 323 (1964).
17. Vrentas, J. S., J. L. Duda, and K. G. Bargeron, *ibid.*, **12**, 837 (1966).

Manuscript received February 1, 1968; revision received April 1, 1968; paper accepted April 4, 1968. Paper presented at AIChE New York City meeting.

The Laminar Boundary Layer on a Moving Continuous Flat Sheet Immersed in a Non-Newtonian Fluid

V. G. FOX, L. E. ERICKSON, and L. T. FAN

Kansas State University, Manhattan, Kansas

The laminar boundary layers on a moving continuous flat surface in non-Newtonian fluids characterized by the power law model are investigated using exact and approximate methods. Both pseudoplastic and dilatant fluids are considered. Numerical solutions of the boundary-layer equations are obtained for values of the parameter n in the power law model ranging from 0.1 to 2.0. An integral solution of the momentum equation, which can be used to obtain values of the dimensionless shearing stress that are in good agreement with the exact values, is developed. An integral solution to the energy equation is also presented.

Non-Newtonian fluids are becoming increasingly important industrially. This increasing importance supplies the motivation for solving the boundary-layer equations for non-Newtonian fluids. In this paper the laminar boundary layer on a moving continuous flat surface is investigated for the case of a purely viscous fluid and zero transverse velocity at the surface. The boundary layer momentum equation is solved by an exact method and also by an integral method. Solutions for the boundary layer energy equation are obtained by an integral method. The boundary layer on a moving continuous surface in a Newtonian fluid was previously investigated (*9, 11*). However, to the best of the authors' knowledge, no such investigation has been carried out for a non-Newtonian fluid.

The non-Newtonian fluid model used in this study is the power law model (Ostwald-de Waele fluid) with the parameters defined by

$$\tau = -\left\{K\left|\sqrt{\frac{1}{2}(\Delta:\Delta)}\right|^{n-1}\right\}\Delta \qquad (1)$$

Both pseudoplastic and dilatant fluids are considered and solutions of the boundary-layer equations are obtained for values of the parameter, n, from 0.1 to 2.

The power law model, Equation (1), has been shown to be valid for a large class of non-Newtonian fluids (*1, 3*). In order to develop the expression for τ_{yx},

$$\tau_{yx} = -K\left|\frac{\partial u}{\partial y}\right|^{n-1}\frac{\partial u}{\partial y} \qquad (2)$$

from Equation (1) it is necessary to assume that $\partial u/\partial y$ is much larger than all other velocity gradients. This is the

V. G. Fox is at the University of Denver, Denver, Colorado.

same assumption that is used in deriving the boundary-layer momentum equation.

Acrivos, Shah, and Peterson (*1*) have studied a similar problem for flow past external surfaces. Their statements about the limitations of the power law in the boundary-layer theory apply equally well to the case of continuous moving surfaces.

For fluids characterized by $n < 2$, the characteristic Reynolds number for a power law fluid,

$$N_{Re} = \frac{\rho U_f^{2-n} x^n}{K} \tag{3}$$

can be made as large as one pleases by increasing the velocity of the moving surface, U_f. Since a large Reynolds number is a prerequisite of flow of the boundary layer type, the boundary-layer equations will be valid for high plate velocities.

For $n > 2$ the situation is reversed. Although this case is mathematically interesting no real fluids have been found that can be characterized by values of n in this range.

EXACT SOLUTION

Consider a steady, two dimensional, incompressible flow on a continuous flat surface moving with a constant velocity in a fluid medium at rest as shown in Figure 1. The adopted frame of axes is stationary with its center point (at $x = 0$) located at the slot. The positive x axis extends parallel to the surface and in the direction of its motion. For the upper part of the surface the positive y axis originates at the surface ($y = 0$) and extends upward. For flow next to a moving continuous surface, $\partial u/\partial y \leq 0$. Equation (2) can, therefore, be written as

$$\tau_{yz} = K\left(-\frac{\partial u}{\partial y}\right)^n \tag{4}$$

Using this relationship, the momentum boundary-layer equation becomes

$$u\frac{\partial u}{\partial x} + v\frac{\partial u}{\partial y} = \frac{-K}{\rho}\frac{\partial}{\partial y}\left(-\frac{\partial u}{\partial y}\right)^n \tag{5}$$

The boundary conditions are

$$u = U_f,\ v = 0 \quad \text{at} \quad y = 0 \tag{6}$$

$$u \to 0 \quad \text{as} \quad y \to \infty \tag{7}$$

$$u = 0 \quad \text{at} \quad x = 0 \tag{8}$$

A stream function, ψ, defined by

$$u = \frac{\partial \psi}{\partial y}, \quad v = -\frac{\partial \psi}{\partial x} \tag{9a}$$

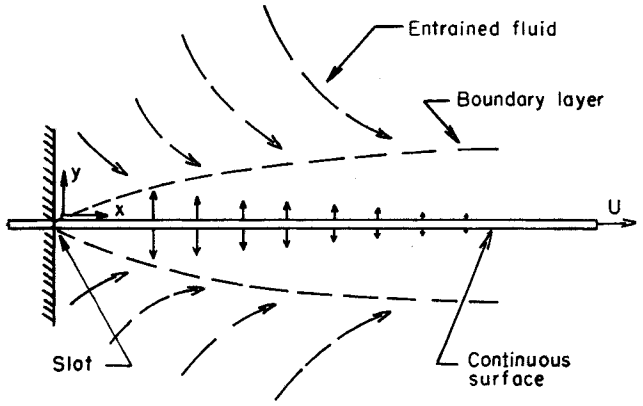

Fig. 1. Boundary layer on a moving continuous flat surface.

and of the form

$$\psi = \left\{\frac{yU_f}{\eta}\right\} f(\eta) \tag{9b}$$

with η defined as

$$\eta = y\left\{\frac{\rho U_f^{2-n}}{Kx}\right\}^{\frac{1}{n+1}} \tag{10}$$

is introduced to satisfy the equation of continuity. The equations of continuity and momentum can now be transformed into a single ordinary differential equation

$$n(n+1)f''' - f(-f'')^{2-n} = 0 \tag{11}$$

with the boundary conditions,

$$f = 0 \quad \text{at} \quad \eta = 0$$

$$f' = 1 \quad \text{at} \quad \eta = 0 \tag{11a}$$

$$f' \to 0 \quad \text{as} \quad \eta \to \infty$$

Klamkin (*6*) generalized a procedure first set forth by Topfer (*10*) for changing boundary value problems into initial value problems. However, the boundary conditions on Equation (11) are not quite of the form that allows such a transformation, and Equation (11) must be solved by a trial and error procedure if forward integration is to be used. Another difficulty associated with Equation (11) is that the range of the independent variable is infinite. For any numerical solution this necessitates choosing a particular finite value of the independent variable at which the boundary conditions may be approximately satisfied.

The problem associated with the infinite range of the independent variable can be surmounted by a transformation suggested by Cohen and Reshotko (*2*). The transformation of Equation (11) is accomplished by substituting $g(\xi)$ for $f'(\eta)$ where ξ is defined by

$$\xi \equiv f'(\eta) \tag{12}$$

Equation (12) allows the boundary conditions expressed at $\eta = 0$ to be expressed at $\xi = 1$ and the boundary condition at $\eta \to \infty$ at $\xi = 0$. The transformation of Equation (11) from η space to ξ space follows.

The chain rule of differential calculus gives

$$\frac{d}{d\eta} = \frac{d\xi}{d\eta}\frac{d}{d\xi} = f''(\eta)\frac{d}{d\xi} = g(\xi)\frac{d}{d\xi} \tag{13}$$

Using the above relation, one can write

$$f''' = \frac{df''}{d\eta} = g(\xi)\frac{dg}{d\xi} = g(\xi)\,g'(\xi) \tag{14}$$

and

$$f = \int_0^\eta f'(t)\,dt = \int_1^\xi \frac{\xi_1 d\xi_1}{g(\xi_1)} \tag{14a}$$

Putting these results into the momentum equation, Equation (11), gives

$$-n(n+1)(-g)^{n-1}\frac{dg}{d\xi} = \int_1^\xi \frac{\xi_1 d\xi_1}{g(\xi_1)} \tag{15}$$

Separating variables and integrating yield

$$(n+1)(-g)^n = -\int_0^\xi \left\{\int_{\xi_1}^1 \frac{\xi_2 d\xi_2}{g(\xi_2)}\right\} d\xi_1 \tag{16}$$

The limits on the integrals have been chosen so that $g = 0$ at $\xi = 0$.

The integrals in Equation (16) were evaluated by Picard's method of successive approximations (*5, 8*).

An asymptotic analysis presented in a later section

predicts that $\lim_{\eta\to\infty} f(\eta) \to \infty$ for $n \leq 0.5$. Thus the integrand of the outer integral of Equation (16),

$$\int_{\xi_1}^{1} \frac{\xi_2 d\xi_2}{g(\xi_2)}$$

may be undefined at $\xi_1 = 0$ for $n \leq 0.5$. This difficulty can be overcome by rewriting the equation for $dg/d\xi$ [Equation (15)] as

$$\frac{dg}{d\xi} = -\frac{1}{n(n+1)}(-g)^{1-n}\int_1^{\xi} \frac{\xi_1 d\xi_1}{g(\xi_1)}$$

Integrating and applying the boundary condition, $g = 0$ at $\xi = 0$, yield

$$g(\xi) = \frac{1}{n(n+1)}\int_0^{\xi} [-g(\xi_1)]^{1-n}\int_{\xi_1}^{1}\frac{\xi_2 d\xi_2}{g(\xi_2)}\, d\xi_1 \tag{17}$$

Equation (17) was used to obtain values for $g(\xi)$ for $n < 1$.

The primary boundary layer property, the shearing stress at the wall, as well as the momentum thickness can be obtained from the momentum equation in the velocity plane. The dimensionless shearing stress at the wall is obtained from Equations (4), (9), and (10) as

$$\bar{\tau}_w = \frac{\tau_w}{KU_f^n}\left\{\frac{\rho U_f^{2-n}}{Kx}\right\}^{\frac{-n}{n+1}} = (-f_w'')^n = [-g(1)]^n \tag{18}$$

The momentum thickness is obtained from Equations (9) and (10) as

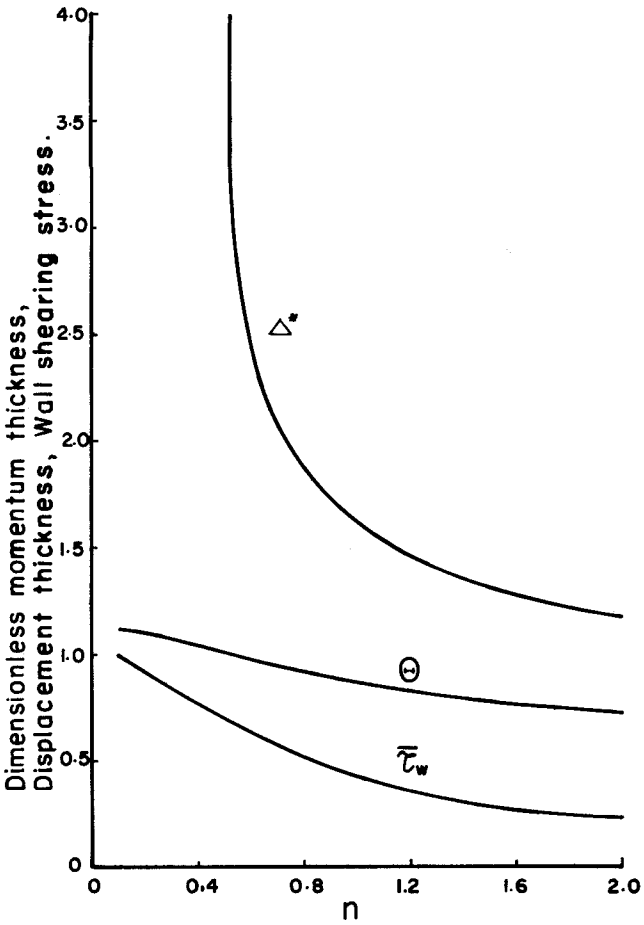

Fig. 2. Boundary layer parameters for a moving continuous flat surface immersed in a power law fluid.

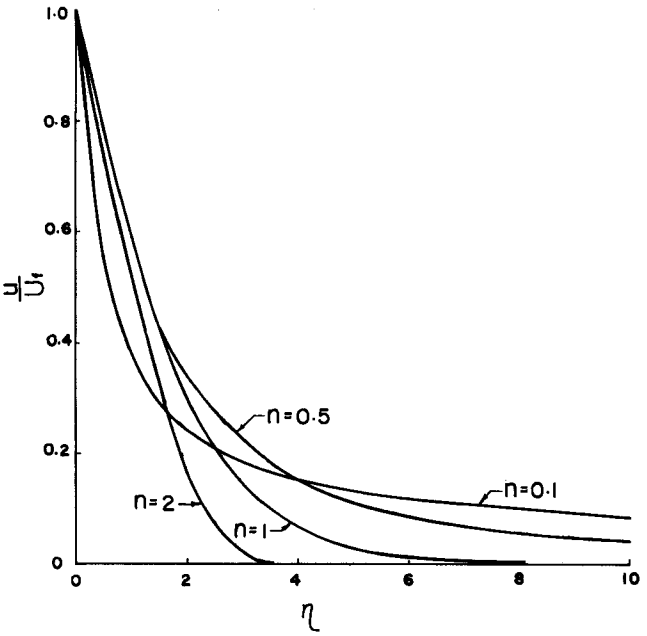

Fig. 3. Velocity profiles for a continuous flat surface immersed in a power law fluid.

$$\theta_m = \frac{1}{U_f^2}\int_0^{\infty} u^2 dy = \left\{\frac{\rho U_f^{2-n}}{Kx}\right\}^{\frac{-1}{n+1}}\int_0^{\infty}(f')^2 d\eta \tag{19}$$

Completing the integral of Equation (19) yields an expression for the dimensionless momentum thickness, Θ, as

$$\Theta = \theta_m\left\{\frac{\rho U_f^{2-n}}{Kx}\right\}^{\frac{1}{n+1}} = (n+1)(-f_w'')^n = (n+1)[-g(1)]^n \tag{20}$$

Furthermore, the dimensionless displacement thickness, Δ^*, can be written in terms of the dimensional displacement thickness, δ^* where

$$\delta^* = \int_0^{\infty}\frac{u}{U_f}dy = \left\{\frac{\rho U_f^{2-n}}{Kx}\right\}^{\frac{-1}{n+1}}\int_0^{\infty} f' d\eta$$

as

$$\Delta^* = \delta^*\left\{\frac{\rho U_f^{2-n}}{Kx}\right\}^{\frac{1}{n+1}} = f\Big|_{\eta\to\infty} = -\int_0^1 \frac{\xi d\xi}{g(\xi)} \tag{21}$$

The integral appearing in the equation for Δ^* is similar to the inner integral appearing in Equation (16). The value for this integral is determined in the process of solving Equation (16).

Values for the dimensionless shearing stress at the wall, momentum thickness, and displacement thickness are shown as functions of η in Figure 2. Velocity profiles for $n = 0.1$, 0.5, 1, and 2 are plotted in Figure 3. The profile for $n = 1$ corresponds to the Newtonian (4) and the computation of the profile for $n = 2$ requires a special consideration described later.

ASYMPTOTIC BEHAVIOR OF $f(\eta)$ AS $\eta\to\infty$

An asymptotic form for f, f', and f'' can be obtained from a solution of Equation (11),

$$n(n+1)f''' - f(-f'')^{2-n} = 0$$

for large values of η. Since f' which represents the dimensionless velocity is always greater than zero and since

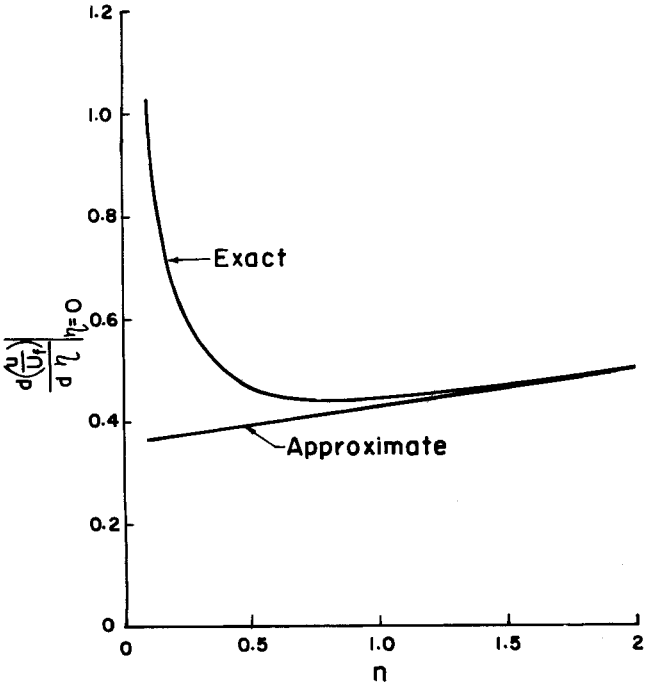

Fig. 4. Comparison of exact and approximate dimensionless velocity gradients for continuous moving flat surfaces immersed in power law fluids.

$f' \to 0$ as $\eta \to \infty$, one can assume that f is bounded. The asymptotic value of f (denoted $\tilde{f}$) can be written as

$$\tilde{f}(\eta) = M + \tilde{f}_1(\eta) \tag{22}$$

where M is the least upper bound of $\tilde{f}$. Note that $\tilde{f}_1(\eta) < 0$.

Equation (11) becomes for large values of η

$$n(n+1)\tilde{f}_1''' - M(-\tilde{f}_1'')^{2-n} = 0 \tag{23}$$

Solutions of Equation (23) can be obtained by standard techniques (*1*). However, the results of interest are

$$\tilde{f}_1' = \frac{(n+1)}{M}\left\{\frac{(1-n)M\eta}{n(n+1)} + C_1\right\}^{\frac{n}{n-1}} + C_3, \qquad 1 < n \leq 2 \tag{24}$$

and

$$\tilde{f}_1 = \left(\frac{(n+1)}{M}\right)^2\left(\frac{-n}{2n-1}\right)\left\{\frac{(1-n)M\eta}{n(n+1)} + C_1\right\}^{\frac{2n-1}{n-1}} + C_4, \quad 0 < n < 0.5 \tag{25}$$

$$\tilde{f}_1 = \left(\frac{n}{1-n}\right)\left(\frac{(n+1)}{M}\right)^2 \ln\left\{C_1 + \frac{(1-n)M\eta}{n(n+1)}\right\} + C_5, \quad n = 0.5 \tag{26}$$

Equation (24) shows that as $\eta \to \infty$, the magnitude of the term containing η becomes very large. Therefore, for $1 < n \leq 2$, a function for the asymptotic value of f that satisfies Equation (11)

$$n(n+1)f''' - f(-f'')^{2-n} = 0$$

along with the boundary condition

$$f' \to 0 \quad \text{as} \quad \eta \to \infty$$

cannot be found. An analytical solution of Equation (11) for $n = 2$ leads to the same result.

In order for the solution to the boundary layer equation, Equation (11), to be meaningful for values of the parameter $1 < n \leq 2$ the boundary condition imposed on f',

$$f' \to 0 \quad \text{as} \quad \eta \to \infty,$$

must be changed to

$$f' = 0 \quad \text{at} \quad \eta = \eta_c$$
$$f'' = 0 \quad \text{at} \quad \eta = \eta_c$$

where η_c is a constant. The numerical values of exact velocity profiles given in Figure 8 are based on this set of the boundary conditions. This phenomenon of a finite boundary layer thickness has not been encountered in the study of Newtonian fluids. Physically, it is doubtful that any real fluid behaves in this manner. The result of a finite boundary layer can probably be attributed to the failure of the power law model for dilatant fluids to describe properly the relationship between the stress tensor and the velocity gradient over the range of the velocity gradient encountered. Equations (25) and (26) show that f_1 does not approach zero as η approaches infinity for $n \leq 0.5$. The assumption made in deriving these equations was that f_1 is bounded; however, this assumption has been contradicted for $n \leq 0.5$ and is not entirely unexpected. At low values of n the power law model predicts high apparent viscosities at low shear rates. Thus plug flow is approached in the boundary layer and the boundary layer becomes very thick.

APPROXIMATE SOLUTION

The behavior of a laminar boundary layer on a flat sheet immersed in a power law non-Newtonian fluid can be approximated by the use of an integral momentum method. The method used here is the traditional Pholhausen method with a polynomial profile.

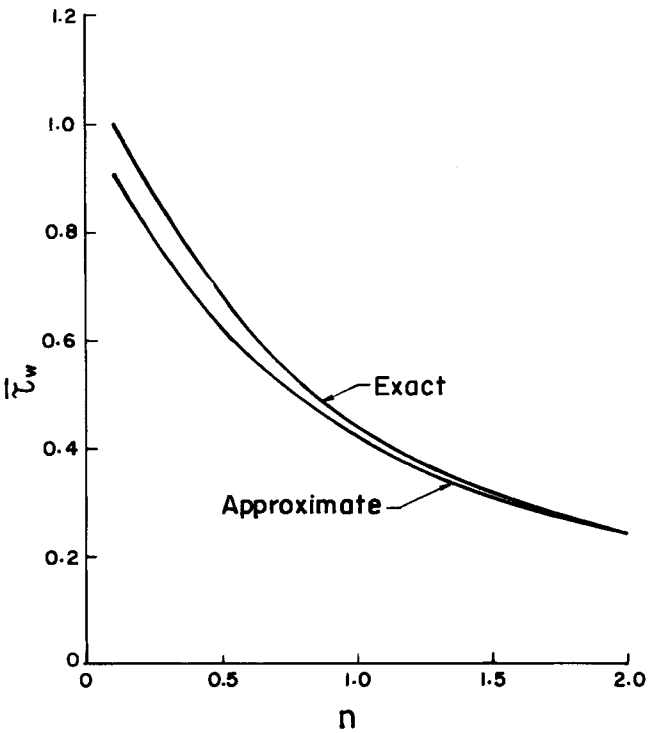

Fig. 5. Comparison of exact and approximate dimensionless wall shearing stress for continuous flat surfaces immersed in power law fluids.

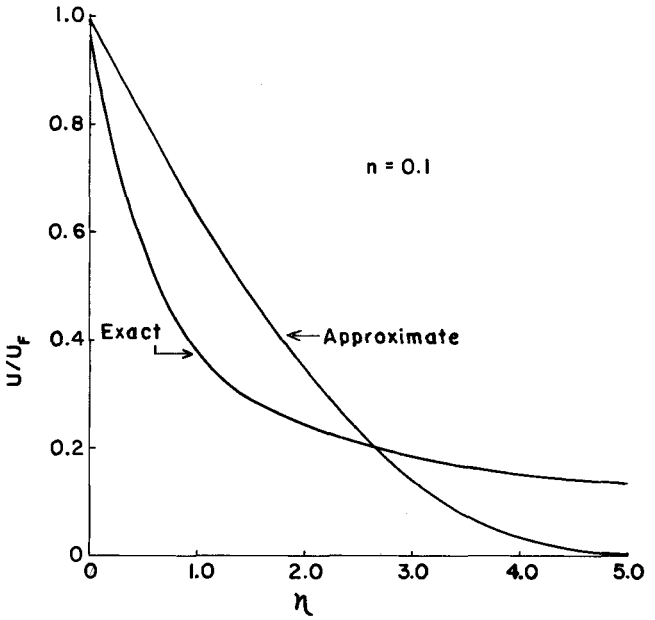

Fig. 6. Comparison of the exact velocity profile with the profile obtained using the integral approximation for fluids with $n = 0.1$.

Integration of the continuity equation gives

$$v = -\int_0^y \left(\frac{\partial u}{\partial x}\right) dy_1 \tag{27}$$

Substituting this expression for v into Equation (5), multiplying the resulting expression by (dy) and subsequently integrating from $y = 0$ to $y = h$, where h is outside the momentum boundary layer, give

$$\frac{d}{dx}\int_0^h u^2 dy = \frac{K}{\rho}\left(-\left.\frac{\partial u}{\partial y}\right|_w\right)^n \tag{28}$$

The velocity profile approximated by a fourth-order polynomial

$$\frac{u}{U_f} = 1 - 2\left(\frac{y}{\delta}\right) + 2\left(\frac{y}{\delta}\right)^3 - \left(\frac{y}{\delta}\right)^4 \tag{29}$$

satisfies the boundary conditions

$$\begin{aligned} u &= U_f && \text{at } y = 0 \\ \frac{\partial^2 u}{\partial y^2} &= 0 && \text{at } y = 0 \\ u &= 0 && \text{at } y = \delta \\ \frac{\partial u}{\partial y} &= 0 && \text{at } y = \delta \\ \frac{\partial^2 u}{\partial y^2} &= 0 && \text{at } y = \delta \end{aligned} \tag{30}$$

This velocity profile gives, when substituted into Equation (28),

$$\delta^n \frac{d\delta}{dx} = 2^n \left\{\frac{126}{23}\right\} \frac{K}{\rho U_f^{2-n}} \tag{31}$$

The boundary condition for this expression is

$$\delta = 0 \qquad \text{at } x = 0$$

The solution of Equation (31) is

$$\delta = \left\{2^n (n+1)\left[\frac{K}{\rho U_f^{2-n}}\right]\left(\frac{126}{23}\right)\right\}^{\frac{1}{n+1}} x^{\frac{1}{n+1}} \tag{32}$$

The dimensionless velocity gradient at the wall, $\partial(u/U_f)/\partial\eta$, may be determined from Equations (10) and (29) as

$$\frac{\partial(u/U_f)}{\partial\eta} = \frac{\partial(u/U_f)}{\partial y}\frac{\partial y}{\partial\eta} = -\frac{2}{\delta}\left\{\frac{Kx}{\rho U_f^{2-n}}\right\}^{\frac{1}{n+1}}$$

Substituting the expression for δ, Equation (32), gives

$$\frac{\partial(u/U_f)}{\partial\eta} = -2\left\{\frac{23}{(n+1)(2^n)126}\right\}^{\frac{1}{n+1}} \tag{33}$$

The dimensionless shear stress at the wall becomes, from Equation (4), the initial equality of Equation (18), and Equation (33),

$$\bar{\tau}_w = 2^n\left\{\frac{23}{(n+1)(2^n)126}\right\}^{\frac{n}{n+1}} \tag{34}$$

These quantities are shown in Figures 4 and 5 respectively and in these figures they are also compared with exact values. Figures 6, 7, and 8 show a comparison of the approximate velocity profiles and the exact profiles for n equal 0.1, 1, and 2, respectively.

HEAT TRANSFER FROM AN ISOTHERMAL MOVING FLAT SURFACE

A similarity solution for the thermal or energy boundary-layer equation is not possible for non-Newtonian fluids described by the power law (7). Therefore, other methods must be considered for establishing rates of heat transfer and temperature profiles. Once the velocity distribution has been obtained, the two components of the fluid velocity, u and v, can be substituted into the thermal boundary-layer equation. A solution to this equation will yield temperature profiles and the rate of heat transfer at the isothermal surface. Closed form solutions to this linear partial differential equation are not possible and finite difference techniques must be used for an exact solution. The integral technique used for the approximate solution of the energy equation for Newtonian fluids can also be used to obtain approximate results for the case of non-New-

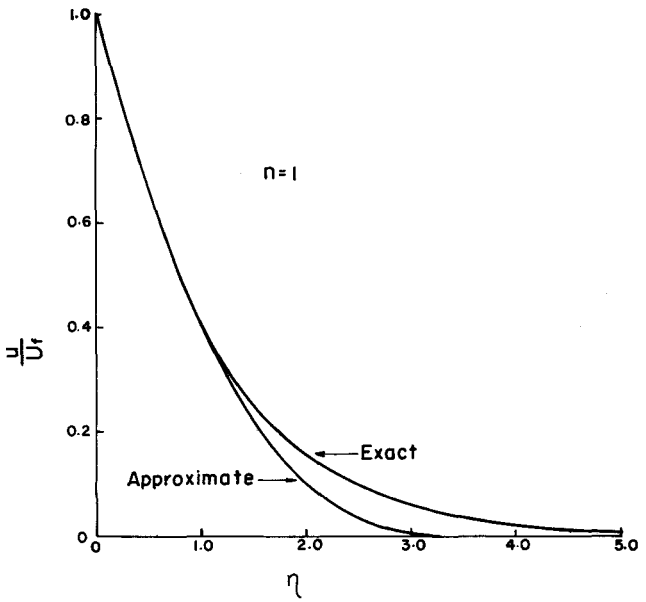

Fig. 7. Comparison of the exact velocity profile with the profile obtained using the integral approximation for fluids with $n = 1$.

tonian fluids.

The energy integral equation for non-Newtonian fluids is identical to the energy integral equation for Newtonian fluids, which is (*4, 11*)

$$U_f \frac{d}{dx} \int_0^{\delta_T} \left(\frac{u}{U_f}\right) \theta \, dy = -\alpha \left(\frac{\partial \theta}{\partial y}\right)_w \tag{35}$$

where

$$\theta = \frac{T - T_\infty}{T_w - T_\infty} \tag{36}$$

and δ_T is the thermal boundary layer thickness. The velocity profile given by Equation (29) may be used in Equation (35) together with the temperature profile.

$$\theta = 1 - 2\left(\frac{y}{\delta_T}\right) + 2\left(\frac{y}{\delta_T}\right)^3 - \left(\frac{y}{\delta_T}\right)^4 \tag{37}$$

which is chosen to satisfy the appropriate boundary conditions for the isothermal moving plate (*4, 11*).

After substituting Equations (29) and (37) into the energy integral equation, Equation (35), and performing the indicated integration, one obtains

$$(\Delta)\delta \frac{d}{dx}\left[\delta\left(\frac{3}{10}\Delta - \frac{2}{15}\Delta^2 - \frac{73}{140}\Delta^4 - \frac{7}{60}\Delta^5 + \frac{1}{9}\Delta^6\right)\right] = \frac{2\alpha}{U_f} \tag{38}$$

where Δ is the ratio of the thermal boundary layer thickness to the momentum boundary layer thickness, that is,

$$\Delta = \frac{\delta_T}{\delta} = \Delta(x) \tag{39}$$

This equation is subject to the boundary condition,

$$\delta_T = 0 \qquad \text{at} \qquad x = 0 \tag{40}$$

Since values of the Prandtl number for non-Newtonian fluids are generally high, it is reasonable to assume that the thermal boundary layer will be thinner than the momentum boundary layer and Δ will be small. Dropping all terms of order Δ^2 or higher in Equation (38) gives

$$(\Delta)\delta \frac{d}{dx}(\Delta)\delta = \frac{20}{3}\left(\frac{\alpha}{U_f}\right) \tag{41}$$

subject to

$$\delta_T = 0 \qquad \text{at } x = 0 \tag{42}$$

Integration yields

$$(\Delta^2)\delta^2 = \frac{40}{3}\left(\frac{\alpha x}{U_f}\right) \tag{43}$$

or

$$\delta_T = \left(\frac{40\alpha x}{3U_f}\right)^{1/2} \tag{44}$$

The temperature gradient at the continuous moving surface can be calculated from Equation (37) as

$$\left(\frac{d\theta}{dy}\right)_w = -\left(\frac{3U_f}{10\alpha x}\right)^{1/2} \tag{45}$$

Thus, when Δ is small and the dropping of higher order terms in Equation (39) can be justified, the heat transfer to or from the moving continuous surface does not depend on the flow behavior index, n.

The following calculations show that for many physical problems the assumption of $\Delta < 1$ is indeed justified.

Substituting the value found for δ in Equation (32) into Equation (43) gives

$$\Delta = \left(\frac{40}{3}\right)^{1/2}\left(\frac{23}{(2n)(126)(n+1)}\right)^{\frac{1}{n+1}} \alpha^{1/2} U_f^{\frac{3(1-n)}{2(n+1)}} \left(\frac{\rho}{K}\right)^{\frac{1}{n+1}} x^{\frac{n-1}{2(n+1)}} \tag{46}$$

If the Prandtl number for power law fluids is defined as

$$N_{Pr} = \frac{C_p U_f \rho x}{k N_{Re}^{\frac{2}{1+n}}}$$

then

$$\Delta = \left(\frac{1}{N_{Pr}^{1/2}}\right)\left(\frac{40}{3}\right)^{1/2}\left[\frac{23}{2^n(126)(n+1)}\right]^{\frac{1}{n+1}} \tag{47}$$

In order to show the dependence of the ratio of the boundary layer thickness, Δ, on x it is convenient to multiply and divide the right side of Equation (47) by $x^{1-n/2(1+n)}$ giving

$$\Delta = \frac{1}{(N_{Pr} x^{\frac{n-1}{1+n}})^{1/2}}\left(\frac{40}{3}\right)^{1/2}\left[\frac{23}{2^n(126)(n+1)}\right]^{\frac{1}{n+1}} x^{\frac{n-1}{2(1+n)}} \tag{48}$$

For values of

$$N_{Pr} x^{\frac{n-1}{1+n}} = \frac{C_P (U_f^{3n-3} \rho^{n-1} K^2)^{\frac{1}{1+n}}}{k} > 100$$

an analysis can be made (*5*), which shows that for

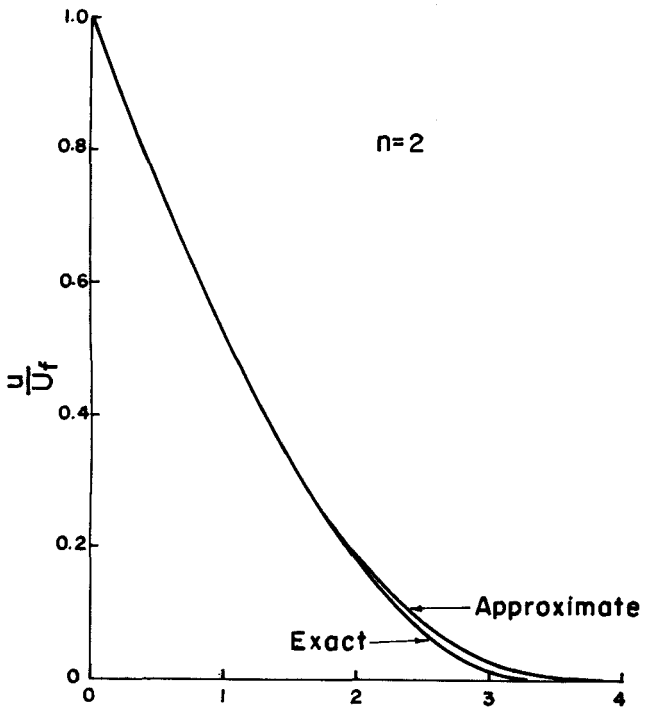

Fig. 8. Comparison of the exact velocity profile with the profile obtained using the integral approximation for fluids with $n = 2$.

pseudoplastic fluids

$$\Delta < 1 \qquad \text{for} \qquad x > 0.002$$

and for dilatant fluids in the range $1 < n \leq 2$

$$\Delta < 1 \qquad \text{for} \qquad x < 10^6$$

Thus Equation (48) is valid over essentially all of the moving surface. Numerical integration of Equation (46) confirms this result.

DISCUSSION AND CONCLUSIONS

The results of the numerical solution of the boundary-layer momentum equation, which are plotted in Figure 2, show that the dimensionless momentum thickness Θ, the dimensionless shearing stress at the wall, $\bar{\tau}_w$, and the dimensionless displacement thickness, Δ^*, increase as the parameter n in the power law model decreases. When these results are compared with the results of Acrivos, et al. (*1*) for a flat plate with a leading edge, one sees that the changes in the dimensionless momentum thickness with changes in n are similar; however, for every value of n considered, the dimensionless momentum thickness for the moving continuous flat surface is larger than the corresponding result listed by Acrivos, et al. (*1*).

This difference in the results is due to the fundamental differences between the two problems (*4*, *9*). In particular, fluid is entrained by the boundary layer for the case of the moving continuous surface while in the case of the finite stationery surface studied by Acrivos, et al. fluid is ejected from the boundary layer. This fact may account for the thicker boundary layer encountered on moving continuous surfaces.

As shown in Figure 2, the value of the dimensionless displacement thickness, Δ^*, increases rapidly as n decreases toward 0.5. Although the asymptotic analysis predicts that Δ^* approaches infinity as n approaches 0.5, the numerical integration of Equation (21) gives a value close to 4 when $n = 0.5$. However, the numerical values of Δ^* computed for $n = 0.25$ and $n = 0.1$ are much larger than this and it is probable that Δ^* is infinite for $n < 0.5$.

The integral solution to the momentum equation gives rise to values of the dimensionless shearing stress at the wall which are in good agreement with the exact solution. This is in spite of the fact that for $n \leq 0.5$, as shown in Figure 4, the predicted value of $\partial u/\partial y|_w$ based on the integral solution is a poor approximation to the exact value. Acrivos, et al. (*1*) also found that for small values of n the integral method gives acceptable results for the dimensionless shearing stress, but that it does not give acceptable results for $\partial u/\partial y|_w$. An examination of Figures 6, 7, and 8 shows that the assumed velocity profile which is used with the integral method is a good approximation for $n = 1$ and $n = 2$, but that it is very poor for $n = 0.1$.

A simplified integral solution of the energy equation is presented and shown to be a valid integral solution over most of the continuous surface. One should keep in mind, however, that the solution presented is only an integral solution and in particular the solution is dependent on a velocity profile that does not predict the term $\partial u/\partial y|_w$ for $n \leq 0.5$ very well. The question of the validity of the integral procedure cannot be resolved completely until a solution for the problem has been obtained by a method more exact than the integral method presented here.

NOTATION

A = constant of integration, dimensionless
B = constant of integration, dimensionless
C_p = heat capacity of fluid, L^2/t^2T
$C, C_1, C_2, \ldots$ = constants of integration, dimensionless
f = stream function in terms of η, dimensionless
$\tilde{f}$ = asymptotic representation for f, dimensionless
$\tilde{f}_1$ = second order term in asymptotic representation of f, dimensionless
g = dimensionless velocity gradient in terms of ξ
K = parameter in power law model, M/Lt^{2-n}
k = thermal conductivity, ML/t^3T
M = least upper bound of f, dimensionless
N = large positive number
N_{Pr} = non-Newtonian Prandtl number, dimensionless
N_{Re} = non-Newtonian Reynolds number, dimensionless
n = parameter in the power law model, dimensionless
T = temperature of the fluid, T
U_f = velocity of the continuous moving surface, L/t
u = fluid velocity component in the x direction, L/t
v = fluid velocity component in the y direction, L/t
x = coordinate of Cartesian system of axes, L
y = coordinate of Cartesian system of axes, L

Greek Letters

α = $k/\rho C_p$, thermal diffusivity, L^2/t
β = $(1/6)^{1/3}$
Δ = δ/δ_T, dimensionless
Δ^* = dimensionless displacement thickness
$\mathbf{A}$ = rate of deformation tensor, L/t^2
δ = thickness of the momentum boundary layer, L
δ_T = thickness of the thermal boundary layer, L
δ^* = displacement thickness, L
ϵ = small positive number, dimensionless
Θ = dimensionless momentum thickness
θ = $(T - T_\infty)/(T_w - T_\infty)$, dimensionless temperature
θ_m = momentum thickness, L
ξ = dimensionless velocity
ρ = fluid density, M/L^3
$\bar{\tau}_w$ = dimensionless shearing stress at the wall
τ = shearing stress, M/Lt^2
ψ = stream function, L^2/t

Subscripts

i = iteration number
w = value taken at fluid solid interface

LITERATURE CITED

1. Acrivos, A., M. J. Shah, and E. E. Peterson, *AIChE J.*, **6**, 312 (1960).
2. Cohen, C. B., and E. Reshotko, in "Recent Advances in Heat and Mass Transfer," J. P. Hartnett, ed., McGraw-Hill, New York (1961).
3. Drew, T. B., and J. W. Hoopes, Jr. ed., "Advances in Chemical Engineering," p. 77, Academic Press, New York (1956).
4. Erickson, L. E., Ph.D. dissertation, Kansas State Univ., Manhattan (1964).
5. Fox, V. G., Ph.D. dissertation, Kansas State Univ., Manhattan (1967).
6. Klamkin, M. S., *SIAM Rev.*, **4**, 43 (1962).
7. Lee, S. Y., and W. F. Ames, *AIChE J.*, **12**, 700 (1966).
8. Nielsen, K. L., "Methods in Numerical Analysis," Macmillan, New York (1960).
9. Sakiadis, B. C., *AIChE J.*, **7**, 26, 221, 467 (1961).
10. Topfer, C., *Z. Math. u. Phys.*, **60**, 397 (1912).
11. Tsou, F. K., Ph.D. thesis, Univ. Minnesota, Minneapolis (1965).

Manuscript accepted November 1, 1967; revision received April 11, 1968; paper accepted April 17, 1968. Paper presented at AIChE St. Louis meeting.